Thermal behaviour of the different parts of almond shells as waste biomass

Eduardo Garzón · Carolina Arce · Angel J. Callejón-Ferre · José M. Pérez-Falcón · Pedro J. Sánchez-Soto

Abstract
The main aim of this study is to investigate the thermal behaviour of the different parts of almond shells produced in an almond industry as a waste biomass. For this purpose, several experiments have been conducted under laboratory conditions. After removing the mature almonds, the waste raw materials subject of this study were treated with distilled water (10 min) and separated in several parts. Taking into account their physical characteristics, they were: (a) complete shells: exocarp, mesocarp and endocarp without grinding (Sample C); (b) ground samples of complete shells, sieved under 0.2 mm (Sample M); (c) hard layers of the endocarp (Sample E); (d) internal layers of the endocarp (Sample I); and (e) mature drupes (Sample P) or skin, being constituted by the flexible part of green colour (fresh form) or yellow (after drying). The thermal behaviour of all these sample materials has been investigated using a laboratory furnace, with determination of ash contents and mass loss by progressive heating (120 min of holding time). Elemental and DTA-TG/DTG analyses of selected sample materials have been carried out. Although a complete study can be very complex, a first approach has been performed in this investigation. Results on thermal decomposition of this biomass waste have been presented to emphasize the main differences between sample materials of almond shells. These results have demonstrated the influence of several parameters, such as the particle size, and previous treatments in the thermal behaviour of the different parts of the almond shells, as showed in this investigation. Structural analysis of almond shells allowed to determine lignin, cellulose and hemicellulose. From the lignin content, it has been predicted the higher heating value (18.24 $MJkg^{-1}$) of this waste as by-product of industrial interest. Other linear correlations to calculate this parameter have been applied with similar results in all these samples.

Keywords Almond shells · Biomass · Thermal behaviour · Wastes · Lignin · Higher heating value

Introduction

The use of biomass to generate energy increased substantially in the European Community, becoming the highest growth renewable energy, which is expected to grow and increase in the next years [1–8]. However, some authors dis-tinguish between natural biomass and products derived from natural materials [7, 8]. It is estimated that between 2014 and 2023 the number of biogas plants from various biomass wastes will increase by about 650 to more than 1450, with a total electrical capacity from 900 MW in 2014 to around 1750 MW by 2023 [9]. On the other hand, the investigation of thermal decomposition of biomass using thermal tech-niques is of wide interest. For instance, sewage sludge using TG/DTA [10] and thermal methods (TG-DSC) to investigate the biomass ashes from wood pellet with different thermal histories [11]. Magdziarz et al. [12] studied the properties of ash generated during sewage sludge combustion by a mul-tifaceted analysis using a variety of analytical techniques. Morales et al. [6] performed a thermal study using elemental analysis and TG–DTA of residues from greenhouse crops plant biomass. Shah et al. [13] studied the biomass resi-due characterization of four different types of walnut shells

for their potential application as biofuels using TG–DTA at three different heating rates.

Recently, Reis et al. [14] have investigated by TG-DTG the combustion properties of potential Amazon biomass waste for use as fuel. These authors considered biomass as "a favourite renewable energy resource for the future because it offers advantages such as transformation into fuels of high volatility and reactivity". Interestingly, the co-pyrolysis of macroalgae and lignocellulosic biomass has been studied by Uzoejinwa et al. [15], showing the synergistic effect of co-pyrolysis parameters on yields. This study would provide valuable information for developing an effective strategy in terms of both recycling and organic waste management. It can be noted that Li et al. [16] reported a TG-DTG and FTIR study on the effect of alkali and alkaline earth metals on co-pyrolysis characteristics of municipal solid waste (MSW) and biomass briquettes. The biomass briquettes, compressed from biomass waste, can be used as suitable auxiliary fuel for MSW because of its lower pollution and lower dust levels with reproducibility compared with fossil fuels. Cruz et al. [17] studied by thermal analysis (TG-DTG) and FTIR the physical–chemical characterization and thermal behaviour of cassava hasvest wastes (hulks, stalks, leaves) for application in thermochemical processes. According to these authors, all the results presented demonstrated the importance of this research and its application to science. A comprehensive review of biomass energy resources, environment and sustainable development has been performed by Omer [18]. This author discussed present and future use of biomass as an industrial feedstock for production of chemicals, fuels and other materials. It is important to remark in this section a review reported by Tripathi et al. [19] on biomass waste utilization in low-carbon products, with implications. These authors focused on a "low-carbon route" for their valorization, reviewing the global availability of biomass wastes and their potential for use a feedstock for the manufacture of high-volume construction materials. Furthermore, Lee et al. [20] published an in-depth overview, with up-to-date information related to bioenergy production from biomass residues and waste, on the recent conversion technologies for transforming biomass residues and waste to bioelectricity and biofuels.

Several classification systems of biomass have been proposed [4, 21–23]. For instance, Ni et al. [23] divided biomass resources into four general categories: (i) energy crops; (ii) agricultural residues and waste; (iii) forestry waste and residues; and (iv) industrial and municipal wastes. Based on origin [4], there are primary, secondary and tertiary wastes and energy crops. Based on properties [4], there are wood and wood fuels, agricultural biomass, aquatic biomass, animal and human wastes, contaminated biomass and industrial biomass, energy crops and biomass mixtures. According to Vargas-Moreno et al. [4], there are two types of process that produce energy from biomass: thermochemical and biochemical/biological. The first one includes direct combustion, pyrolysis, gasification and liquefaction. Combustion or oxidizing the biomass with excess air is the most widely used method. The hot gases produced can be used to generate vapour in heat exchangers and, hence, the production of electricity. As pointed out by Ni et al. [23] and other authors [18–20], biomass can be gasified at high temperatures (above 1000 K). The biomass particles undergo partial oxidation resulting in gas and charcoal production. The charcoal is reduced to H_2, CO, CO_2 and CH_4 with light and heavy hydrocarbons and char. Converting biomass into gaseous and aqueous fuels, electricity and hydrogen is possibly a more efficient way of biomass utilization [15].

On the other hand, the almond industry generates large quantities of waste products as biomass source that need to be recycled or processed [24–26]. Thus, it can be mentioned that world production of almonds was 3.21 million tonnes in 2016, with the USA as the larger producer with 1.8 million tonnes. The Spanish production, in second place, accounts for 202.339 tonnes with a total of harvested area of 544.518 Ha in 2016 [26]. The production of Almería Province (SE Spain) was 44.256 tonnes [26]. Consequently, it is generated a large amount of waste biomass. The almond shell is composed of cellulose, hemicellulose and lignin, and the thermal decomposition of this waste produced several pyrolytic compounds, such as carbon, gases and oils [2, 23–25]. It is of interest for several applications, such as the preparation of pyrolytic liquid fuels, fuel boilers, fuel gas and active carbons [23–25].

In an earlier work, Caballero et al. [24] performed a comparison of the behaviour of almond shells and their fractions of "holocellulose" and lignin, in the pyrolysis process. These authors studied the product yields and reaction kinetics. Chiou et al. [25] studied the torrefaction kinetics of almond shells (*Prunus dulcis*) using ground and sieved samples to produce particles less than 90 μm in size and shells leached with deionized water to remove inorganic species. Ni et al. [23] investigated on biomass gasification for hydrogen production. These authors emphasized the use of almond shells as biomass using a fluidized bed and catalysts of La–Ni–Fe or perovskite (at 800 and 900 °C, respectively) [27, 28]. The hydrogen production via supercritical water gasification of almond shells as catalysts has been investigated by Safari et al. [29]. Sabbatini et al. [30] used almond shells and rice husk as fillers of poly(methyl metacrylate) composite materials. In the same sense, Tasdemir [31] studied the effect of almond shell powder and olive pit on polypropylene.

Other interesting application of waste almond shells is as biosorbent. Activated carbons obtained from almond residues, used for water treatments and purification and separation processes (gaseous or aqueous solution systems and catalysis) are major applications of these materials. Maaloul

et al. [32] extracted and characterized novel biosorbents from almond shells. Maaloul et al. [33] studied the dialysis-free extraction and characterization of cellulose crystals from almond (*Prunus dulcis*). It is an attractive application of waste almond shells as low-cost and eco-friendly sorb-ent material [32–34]. Sometimes, almond shells have been used in domestic heating systems and barbecues [35], but some applications with treatment of the wastes seem of more interest for the preparation of added-value materials [36–40]. For instance, Moussa et al. [37] applied almond (*Prunus amygdalus*) by-products in eco-friendly dyening of textile fabrics. Chen et al. [38] discussed the utilization of almond (*Prunus dulcis*) residues, with particular detail concerning the utilization and especially energy uses of these residues, with an assessment of technology options for biomass processing. Allouch et al. [39] studied by DTA-TG-DTG the thermal behaviour of almond shells, combined with acorn cups, for production of briquettes from roasted fine with promotion of renewable energies. This study showed that the residence time during roasting and the particle size were the determinant factors of the quality of the obtained briquettes in contrast with the direct application of the wastes [35].

Finally, Li et al. [40] performed an investigation of ana-tomical and chemical characteristics of almond shells in order to contribute to better utilization of these wastes as bioresource. These characteristics indicated that almond shells have the capacity to be used for new composites and adsorption materials. In fact, the microscopy morphology of the almond shell wall contains holes of several diameters. Thus, it makes the materials of light density with a "poten-tial of absorption" [32–36, 38, 40].

The objective of the present study is to investigate the thermal behaviour of the different parts (separated before any treatment) of almond shells produced in an industry as a waste biomass (almond shells, variety *marcona*). From the precedent literature review, there are several applications of interest using this waste biomass. For this objective, several experiments have been conducted under laboratory condi-tions. Furthermore, the structural analysis of almond shells provided the content of lignin. From this result, elemental analysis data and ash content, some predictions of the higher heating value of this waste, as by-product of industrial inter-est applied as biomass, have been performed.

Experimental

Materials and sample preparation

The raw material was supplied by the Spanish company Llanos del Almendro (Almería Province, Spain). After removing the mature almonds (*Prunus dulcis, amygda-lus,* variety *marcona*, being this variety the higher quality

Fig. 1 Raw almond shells under study treated in distilled water to be separated in several parts for this study

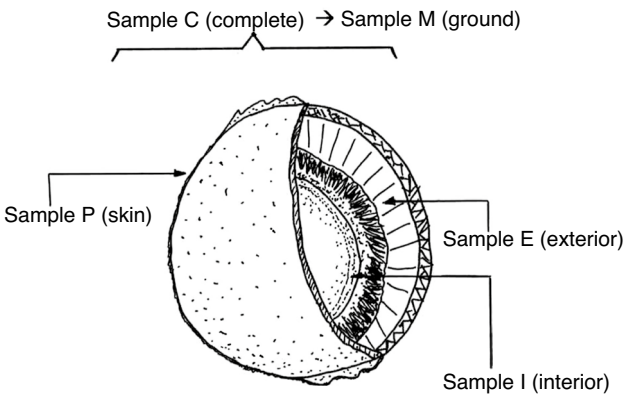

Fig. 2 Scheme of the several parts considered as subject of study in the almond shells as sample materials (samples C, M, P, E and I)

at the World level), the wastes were treated with distilled water rinsed for 10 min in a plastic tray (Fig. 1), being separated by hand in several parts for this study taking into account their physical characteristics, as follows (Fig. 2):

(a) complete shells: exocarp, mesocarp and endocarp without grinding (Sample C);
(b) complete shells ground and sieved under 0.2 mm, resulting a sample similar to industrial processing conditions for further applications (Sample M);
(c) hard layers of the external endocarp (Sample E);
(d) more membranous internal layers of the internal endocarp (Sample I); and
(e) mature drupes (Sample P), or skin, being constituted by the flexible part of green colour (fresh form) or yellow (after drying). In fact, it is not a part of the almond shell, being a protection part during maturation of the almonds.

Figure 3 shows a picture of several selected sample mate-rials, described above, placed in open ceramic crucibles and prepared for thermal treatments in air.

Methods

Thermal treatments and thermogravimetric evolution

All these sample materials were dried in air for 24 h and then treated at 80 °C for 24 h using an oven. The mass loss, in percentage, after heating was determined using ASTM D-7348–08 standard procedure. The ash content was determined according to the UNE-EN 15,403:2011 standard procedure weighing the samples using a balance precision of 0.0001.

Thermal gravimetric experiments using a laboratory furnace (Select, model 2000–367) were carried out in the samples at a heating rate of 20 °C min^{-1} in air (static heat-ing conditions). The samples were treated at 150 ° C for 48 h using open ceramic crucibles (Fig. 3). After this treat-ment, they were cooled using a desiccator and weighed, following a previous procedure to eliminate a part of vola-tile matter [6]. The next thermal treatment was using the samples weighed and treated into the furnace at a heating rate of 6 °C min^{-1} up to 800 °C, with a holding time of 120 min. The crucibles with sample were cooled into the furnace and put into a desiccator at 100 °C and cooled prior to be weighed with balance precision of 0.0001. Triplicate samples were used in these experiments. The average values were obtained with acceptable standard deviations. The mass variation (in percentage) *versus* temperature (ºC) curves were obtained for each sample (Fig. 4).

Fig. 3 Several selected sample materials of almond shells placed in the ceramic crucibles prepared by thermal treatments in air: Sample C, Sample M, Sample I and Sample E

Thermal analysis by TG–DTA

The samples designed C, E, I and P were cut with scissors in small pieces, gently ground using an agate mortar and sieved under 0.2 mm to compare the results with Sample M (ground and sieved under 0.2 mm). A thermal analyzer SDT Q600 (TA Instrument) was used for simultaneous thermal analysis (TG–DTA) using ~ 20 mg of sample and alumina crucibles in air flow (40 cm^3 min^{-1}) at heating rate of 6 °C min^{-1} from 25 to 1000 °C.

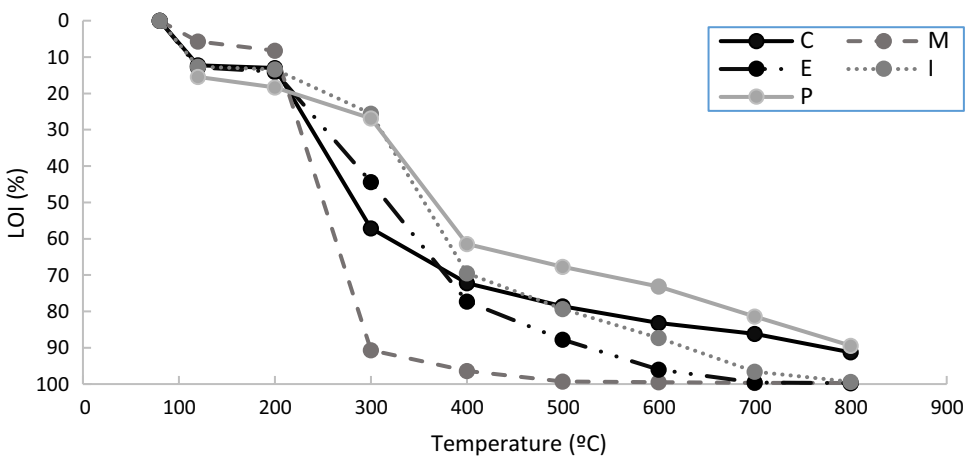

Fig. 4 Mass loss (in mass %, loss on ignition, LOI, %) of the sample materials designed C, M, E, I and P separated from almond shells (see Fig. 2) as increasing heating temperatures

Elemental analysis

An equipment LECO TruSpec, CHN Model, with IR detector for C, S and H and conductivity detector for N, was used for C, H, N and S elemental analysis. The combustion was carried out under 950 to 1300 °C and using pure oxygen atmosphere. Results were obtained by triplicate, and the average was calculated. Reference materials and blank tests were used for equipment calibration [6, 9]. The reference organic compound sulphametazine (certified standard) was employed to check the precision of this equipment. The oxygen content can be calculated taking into account the sum (in mass %) of elemental analysis (C, H, N and S) and the ash content [4, 5, 41, 42].

Structural analysis: determination of lignin, hemicellulose and cellulose

The contents of lignin, cellulose and hemicellulose in selected material samples of almond shells have been determined following the method and protocol proposed by Van Soest et al. [43] implemented at the University of Almería for easy and relative rapid application [4, 5]. From these averaged results of structural analysis of the almond shells, the higher heating values (HHV) in MJ kg^{-1} on dry basis can be estimated according to the linear equation HHV = 0.0864*x*L + 16.6922, where L = Lignin content in mass % on dry basis [1, 5] with no study errors [4].

Results and discussion

Table 1 includes the results of variation of mass loss (in mass loss %) corresponding to sample materials designed C, M, E and I at two temperatures (750 and 950 °C). It can be observed the higher mass loss after heating at 750ºC of the ground sample (Sample M). However, this sample shows an intermediate value at 950 °C as compared with the other samples, being sample I the sample with the highest value. At 950 °C, all the average values reached ~ 90 mass %. It must be noted that the differences are minimum between exterior (Sample E) and interior (Sample I) of the waste almond shells (93.17 mass *versus* 94.69 mass %, respectively).

Figure 4 shows the values in mass loss % as increasing heating temperatures of these sample materials with previous thermal treatments (air drying for 24 h and 80 °C for 24 h). Variations are observed concerning the thermal evolution as increasing heating temperatures. The differences in mass loss are recorded in the range 100–400 °C as compared the samples with "shells" and a relatively larger particle sizes (Samples C, P, E) and ground and sieved (Sample M), as described in experimental section. From 400 °C and higher, the trend of the thermal evolution of the mass loss in all these sample materials is very similar. This variation can be explained associated with a size effect: Sample M is a ground and sieved (0.2 mm) sample and, hence, with a treatment of homogenization, a difference with the rest of samples. A particular case is sample material designed as Sample P, which is composed by the skin of the waste almond shells (Fig. 2), being a protection or support part of the almond shells.

Table 2 shows the results of ash content (on dry basis) of Samples C, M, E and I. The higher ash content was observed in Sample C (10.66 mass %), followed by Sample M (8.71 mass %) with a difference of ~ 2 mass % between sample parts exterior and interior. It should be noted that the ash content (incombustible inorganic remnants of combustion) decreases in the series of sample materials: Sample C through Sample I, from exterior to interior. According to previous results [4], ash contents of different plant biomass vary from less than 1% (in certain wood types) to up to 30–40% (certain greenhouse crop wastes), data in mass % on dry basis. In the case of residues from greenhouses crops plants, the ash content was found of 9.60 mass % [6].

Table 3 includes the results of elemental analysis (C, H, N, S and O) of original samples. These original samples show high values of carbon (in mass %), with maximum of 46.11% in Sample M and minimum of 41.60% in Sample P. The rest of samples show values in the range 45.62 to 43.23%. In general, these values are of the same order than those obtained studying other biomass residues, for instance the results of elemental analysis of biomass (42–54 mass % of dry fuel) as pointed out by Demirbaş [2], or the results reported for greenhouse crops plants [5, 6]. The content of

Table 1 Results of mass variation (LOI = "Loss on ignition" or mass loss after heating at a selected temperature, in mass %) for selected sample materials (Samples C, M, E and I) of almond shells after thermal treatments at 750 and 950 °C

Sample	LOI mass % 750 °C	LOI mass % 950 °C
Sample C	77.53 ± 0.52	89.34 ± 0.42
Sample M	80.70 ± 0.41	91.29 ± 0.33
Sample E	80.44 ± 0.44	93.17 ± 0.22
Sample I	79.68 ± 0.56	94.69 ± 0.15

Table 2 Results of determination of ash content of original selected sample materials designed Samples C, M, E and I

	Sample C	Sample M	Sample E	Sample I
Ash content	10.66 ± 0.32	8.71 ± 0.41	6.83 ± 0.34	5.31 ± 0.23
HHV (MJ/kg)	17.43	17.88	18.32	18.67

Estimation of HHV in MJ kg^{-1} using the equation HHV = 19.914–0.2324xAsh content, as described in [47]

Table 3 Results of elemental analysis (carbon, hydrogen, nitrogen, sulphur and oxygen, in mass %) of original selected sample materials C, M, E, I and P

Sample	% Carbon (C)	% Hydrogen (H)	% Nitrogen (N)	% Sulphur (S)	% Oxygen (O)	HHV (MJ Kg^{-1})
C	45.62 ± 0.10	5.80 ± 0.01	0.07 ± 0.02	…	37.85	17.27
M	46.11 ± 0.08	5.75 ± 0.02	0.14 ± 0.02	…	39.29	17.21
E	44.41 ± 0.12	5.60 ± 0.07	0.15 ± 0.03	…	43.01	16.06
I	43.23 ± 0.34	5.55 ± 0.03	0.33 ± 0.04	…	47.07	15.14
P	41.60 ± 0.26	5.50 ± 0.12	0.52 ± 0.03	…	ND	

The content of oxygen (%) was estimated by difference taking into account the respective ash contents (in mass %), as included in Table 2. ND = Not Determined

The indication … means "below equipment limit detection". The determination of HHV (in MJ kg^{-1}) was performed using the linear correlation HHV = 0.314*x*C + 1.322*x*H − 0.12*x*O − 0.12*x*N + 0.0686S-0.0153*x*Z being Z the fraction of ashes on dry basis, as proposed in reference [49]

hydrogen (mass %) is similar in these almond shells sample materials. It ranges from 5.80 mass % (in Sample C) to 5.50 mass % (in Sample P). The content of nitrogen (in mass %), very scarce, shows more variability in these samples, with a maximum value of 0.33% in Sample I and minimum value of 0.07% in Sample C. From these results and taking into account the ash contents (Table 2), it can be estimated the oxygen content of these sample materials of almond shells (see Table 3). It can be seen that the maximum value of oxygen (in mass %) is reached in Sample I (47.07%) and the minimum in Sample C (37.85%), being slightly high (39.29%) in the ground and sieved sample (Sample M). The values are similar to those found in previous studies on bio-mass residues [2–6]. It should be noted that the differences in oxygen (mass %) between exterior (43.01%) and interior (47.07%), Sample E and Sample I, respectively, are relevant as demonstrated these elemental analyses.

Additional thermal experiments with these samples have been performed using the furnace, and elemental analy-sis of the resultant products has been determined. Table 4 summarizes the main results. Sample C was treated at 800 °C/20 min and 1000 °C/20 min. The content of carbon and hydrogen diminished with these treatments and they are slightly different from the original results (Table 3), with some differences in the hydrogen contents. Sample M was treated using the same thermal conditions as above. In that case, the content of carbon was ~ 80 mass % with a difference of ~ 34 mass % taking into account the carbon content of the original (untreated) sample (Table 3). Differences in hydrogen and nitrogen contents must be also mentioned. The differences between Sample E treated at 800 and 1000 °C/20 min are remarkable, as confirmed the results of carbon content after these thermal treatments and the comparison with these values for the original sample. In the case of Sample I, analogous evolution concerning the elemental analysis can be observed. Finally, Sample P treated at 800ºC for 24 h shows a carbon content of 19.03 mass %, being the original 41.90 mass %, and a lower value of hydrogen con-tent (1.36 mass %) as compared to that value of the original sample (5.50 mass %, Table 3). From these values, it can be evidenced that the conditions of thermal treatment influence these results, in particular in the case of hydrogen (in mass %) as deduced from these elemental analysis results.

All the above results have demonstrated the influence of several parameters, such as the particle size and previous treatments, in the thermal behaviour of the different parts of the almond shells, as studied in this investigation.

The main features of thermal decomposition of these biomass wastes are presented using dynamic conditions of heating (DTA-TG-DTG). As can be observed (Figs. 5 and

Table 4 Results of elemental analysis (Carbon, Hydrogen, Nitrogen, Sulphur and Oxygen, in mass %) of selected sample materials C, M, E, I and P (after several thermal treatments temperatures and holding times) using the laboratory furnace and subsequent cooling

Samples and treatments	% Carbon	%Hydrogen	% Nitrogen	% Sulphur
Sample C 800 °C/20 min	43.57 ± 0.08	1.07 ± 0.04	…	…
Sample C 1000 °C/20 min	40.88 ± 0.09	0.43 ± 0.02	…	…
Sample M 800 °C/20 min	77.69 ± 0.06	1.46 ± 0.04	0.33 ± 0.01	…
Sample M 1000 °C/20 min	81.53 ± 0.08	1.46 ± 0.02	0.17 ± 0.01	…
Sample E 800 °C/20 min	59.66 ± 0.06	1.17 ± 0.08	~ 0.046	…
Sample E 1000 °C/20 min	81.12 ± 0.08	1.87 ± 0.09	~ 0.034	…
Sample I 800 °C/20 min	35.48 ± 0.09	0.97 ± 0.10	~ 0.099	…
Sample I 1000 °C/20 min	51.90 ± 0.07	1.26 ± 0.09	…	…
Sample P 800 °C/24 h	19.03 ± 0.09	1.36 ± 0.08	…	…

The indication … means "below equipment limit detection"

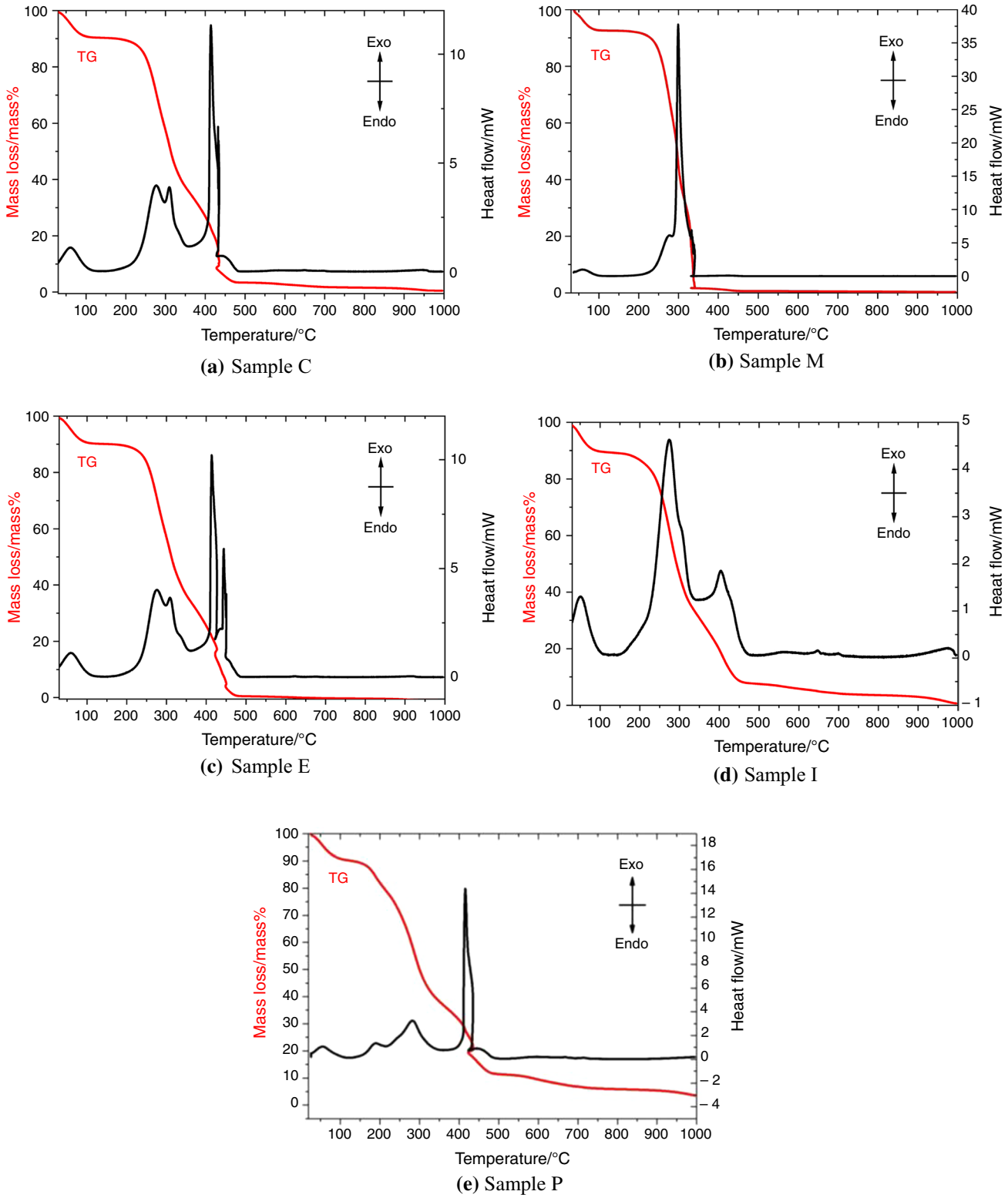

Fig. 5 DTA-TG curves of all these material sample parts separated from waste almond shells, obtained in air flow (heating rate of 6ºC min^{-1}): **a** Sample C, **b** Sample M, **c** Sample E, **d** Sample I and **e** Sample P

6), the thermal decomposition of these samples is complex. It presents several thermal events as observed by DTA-TG (Fig. 5) and TG-DTG (Fig. 6) curves. At a first stage (0-150ºC), there is a slight mass variation with DTG peaks and broad DTA endothermal effects, which can be associated with some light volatile matter, mainly water release. In general, the total mass variation in this temperature range can be estimated 8–10 mass %. The main thermal events in

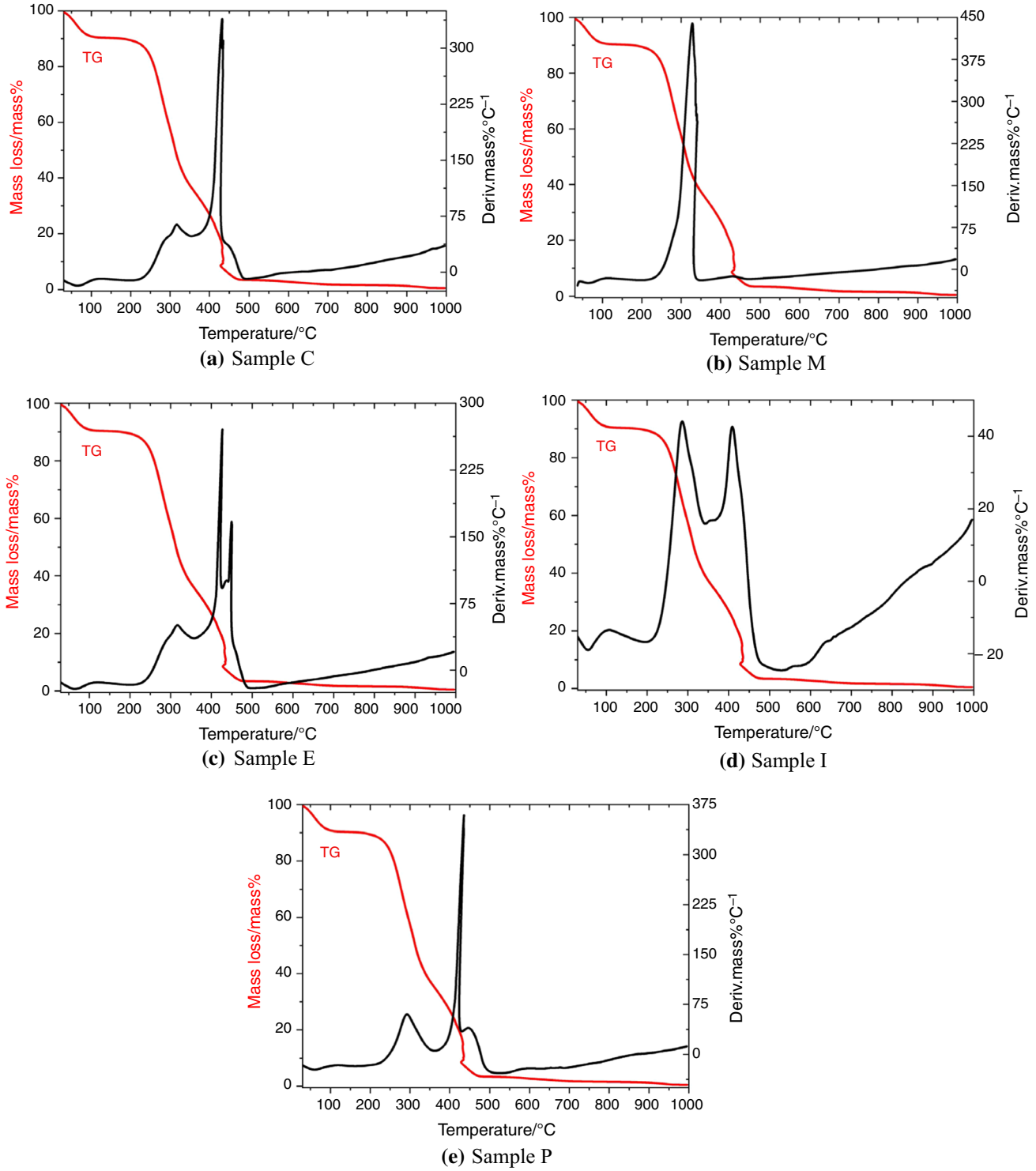

Fig. 6 TG-DTG curves of all these material sample parts separated from waste almond shells, obtained in air flow (heating rate of 6 °C min^{-1}): **a** Sample C, **b** Sample M, **c** Sample E, **d** Sample I and **e** Sample P

these samples occur in the range 200–500 ºC, although in sample M they finished at ~ 350 ºC. It can be an effect of the lower particle size of this sample (ground and sieved under 0.2 mm). Furthermore, in this temperature range, there is a larger mass variation (80–85 mass %) of thermal decomposition with carbonization, showing slight variations in the final ash content of these samples. Samples I and P show lower mass variations, in particular sample P. These mass variations, as detected by a progressive TG increase by heating, are associated with complex overlapping DTG (Fig. 6) curves and several exothermal DTA effects (Fig. 5) of subsequent thermal devolatilization, decomposition and degradation processes. The pyrolysis of the organic matter, cellulose, hemicellulose and lignin (the three components of the almond shells), takes place. Lignin is the more thermostable component of the almond shell whose decomposition takes place slowly over a greater temperature range (~ 400–800 °C) [24, 25, 34, 35]. However, sample M shows a different thermal behaviour as compared with the rest of samples (Figs. 5b and 6b), being associated with an effect of lower particle size, as pointed out above. It can be noted that this thermal evolution is similar to that studied using other biomass residues, for instance greenhouse crops plant biomass [6]. Hemicellulose, cellulose and lignin are the main components of these wastes [5]. It should be noted that volatile material is composed of moisture, light hydrocarbons, CO, CO_2, H_2 and tars. Biomass usually has a high content (48–86 mass % on dry basis) of volatile materials [1–4, 7, 8].

In some more detail (Fig. 6), a first stage (first peak in DTG curves) can be attributed to a water (moisture) release. It takes place at a temperature below ~ 100 °C. The decomposition of the main organic compounds of these parts of the almond shell starts at ~ 175–200 °C. The main mass loss occurs between 250 and 500 °C attributed to a devolatilization/decomposition of hemicellulose and cellulose, being associated in some sample parts of the studied almond shells with second and third peaks in the DTG curve, with a maximum decomposition rate at ~ 300–330 °C. The third stage (third peak in the DTG curve) could be attributed to the degradation of cellulose. In this stage, the maximum decomposition rate occurs at ~ 360 °C or temperatures relatively higher. A possible fourth stage of thermal decomposition can be observed in the TG-DTG curves of some samples, although it appears as a broad peak with smaller intensity, as compared with previous ones. It must correspond to lignin degradation in all these sample parts by progressive heating. Lignin is one of the major components in almond shells, being the more thermostable whose decomposition takes place slowly over a greater temperature range (~ 400–800 °C), as pointed out above.

Caballero et al. [24] found that lignin in almond shells is decomposed across a very wide range of temperatures. Martín-Lara et al. [35] distinguished four stages of pyrolysis as increasing heating temperature studying almond shells (ground to a particle size < 1 mm) in nitrogen atmosphere: (a) first stage of decomposition: associated with moisture (water evaporation); (b) second stage: associated with decomposition of hemicellulose; (c) third stage: associated with cellulose degradation; and (d) fourth stage: associated with lignin degradation. Allouch et al. [39] found three main steps of thermal degradation as studied by DTA: the first one (endothermic), evaporation of moisture from ambient temperature up to 127 °C; the second one (exothermic), devolatilization in the temperature range of 282–398 °C; and the third one (exothermic) occurring between 397–522 °C, final oxidation of the coal.

Table 5 shows a summary of the main decomposition steps of the samples studied in the present investigation related to DTG curves (Fig. 6), identifying the characteristic onset, peak and endset temperatures for each considered sample. Four, five or six decomposition stages can be deduced, although overlapped effects are the main observed feature in these DTG diagrams.

In the present investigation, the main thermal features observed by TG–DTA (Fig. 5), in the material samples, separated from the waste almond shell, studied in this work could be summarized as follows:

Table 5 Summary of the main decomposition steps related to DTG curves identifying the characteristic onset (T_o), peak (T_p) or maximum and endset (T_e) temperatures for each considered sample (C, M, E, I and P). Between parentheses these estimated parameters when the decomposition steps are very broad or overlapped

Thermal decomposition parameters	Sample C	Sample M	Sample E	Sample I	Sample P
T_o, °C	32	30	56	33	61
T_e, °C	161	165	186	156	138
T_p, °C	125	115	128	116	108
T_o,ºC	246	263	244	204	247
T_e, °C	352	344	348	348	348
T_p, °C	287	332	312	278	295
T_o, °C	295	366	284	336	386
T_e, °C	351	486	427	365	448
T_p, °C	322	438	325	348	431
T_o, °C	360	–	394	367	361
T_e, °C	446	–	449	468	480
T_p, °C	432	–	418	409	446
T_o, °C	396	–	366	(536)	(555)
T_e, °C	453	–	472	(566)	(640)
T_p, °C	498	–	436	(558)	(590)
T_o, °C	–	–	(447)	–	–
T_e, °C	–	–	(487)	–	–
T_p, °C	–	–	(466)	–	–

Sample C Previous exothermal DTA effects, with mass loss, centred at ~ 270 and ~ 310 °C. End of the main thermal event of mass loss at ~ 700 °C and DTA exothermal effect centred at ~ 430 °C.

Sample M End of the main thermal event of mass loss at ~ 450 °C and a single DTA exothermal effect centred at ~ 340 °C.

Sample E End of thermal event of mass loss at ~ 600 ºC and two DTA exothermal effects centred at ~ 420 and 450 °C, with a previous DTA broad exothermal effects, with mass loss, centred at ~ 310 and ~ 320 °C.

Sample I End of thermal event of mass loss at ~ 900–1000 ºC and DTA exothermal broad effect centred at ~ 290 °C, with additional DTA exothermal broad effect centred at ~ 420 ºC.

The differences between exterior (Sample E) and interior (Sample I) of the almond shells is relevant according these results.

Sample P. End of thermal event of mass loss at ~ 800 °C and DTA sharp exothermal effect centred at ~ 420 °C and other DTA broad exothermal effects, with mass loss, centred at ~ 290 and ~ 440 °C. This sample is the external part of the almond shells.

However, it is difficult the interpretation of all these ther-mal events. It can be noted that variations in the contents of hemicellulose, cellulose and lignin in almond shells produce some differences in the thermal evolution as observed by thermal analysis (DTA-TG/DTG-DSC) in air and/or nitrogen atmosphere [24, 25, 35, 39].

Table 6 shows the results of determination of hemicellulose, cellulose and lignin in a selected sample material of almond shells waste (Sample M, a sample similar to that used in industrial processing conditions). The results of this structural analysis performed for sample M include the values of four determinations and average values. It should be remarked that the contents of hemicellulose and lignin obtained in the present investigation have been found lower as compared with those found by Yildiz [44] studying almond shells (samples of *Prunus dulcis*). However, the values reported by Demirbas [2] for almond shells (without more data) are different: 28.9 (mass %) hemicellulose, 50.7% cellulose and 20.4% lignin. Caballero et al. [24] reported different values for almond shells (variety marcona, as in the present study): 32 (mass %) hemicellulose, 37 (mass %) cellulose and 27 (mass %) of lignin.

Table 6 Determination of hemicellulose, cellulose and lignin in a selected sample material of almond shells waste (Sample M). The results include the values of four determinations and average values. The prediction of the higher heating values (HHV) is determined on dry basis of this waste (see Experimental section). SD is the standard deviation

Sample M	Hemicellulose (%)	Cellulose (%)	Lignin (%)	HHV (MJ kg^{-1})
1	18.58	36.95	14.30	18.24
2	23.49	32.48	13.83	18.23
3	20.75	33.13	14.36	18.24
4	23.13	30.14	16.71	18.25
Average	21.49	33.18	14.80	18.24
SD	2.29	2.82	1.29	

Taking into account the content of lignin as found in the present work (Table 6), the prediction of the higher heating values (HHV) in MJ/kg^{-1} on dry basis of these wastes can be determined [1]. According to Callejón-Ferre et al. [5], in the analysis of biomass plant remains from greenhouses of Almería (SE Spain), the use of biomass requires that its HHV be known. However, the equipment necessary for this experimental determination is of high-cost. For this reason, mathematical models have been proposed to estimate the HHV [1, 5, 42, 44–49]. The use of simple linear equations is of special interest.

Table 6 shows the results of HHV determined in the present study for sample M. The average of HHV values is representative in this sample of almond shells, being determined a value of 18.24 MJkg^{-1}. It is higher than the values reported by Callejón-Ferre [5] in the analysis of biomass plant remains from Almería (SE Spain). Martín-Lara et al. [35] reported a value of HHV = 16.31 kJkg^{-1} for a sample of almond shell (ground to a particle size < 1 mm), being determined by a calorimeter. Table 2 includes the estimation of HHV for each sample taking into account the previous work of Sheng and Azevedo [47]. These authors based this estimation on the basis of a previous determination of ash content. In the present case, the values obtained using this correlation are close to the average of HHV for sample M as calculated and presented in Table 6. The differences are of 0.40 units of HHV, except for sample C, and being closer for samples M and E. Following the calculations for HHV, in Table 3 has been included a new estimation of HHV taking into account the elemental analysis, presented in Table 3, and the ash content (Table 2), according to the proposed linear correlation described in a previous work by Channivala and Parikh [49]. The values obtained for HHV are close to the average of this result for sample M (Table 6). The rest of samples shows similar values, except for sample I.

Further discussion concerning HHV is of interest. HHV of a material considered as a fuel mainly depends on its carbon content. Chen et al. [38], investigating almond residues, found a value of HHV = 18.2 MJ kg^{-1}. It has been reported energy content, using the parameter HHV, for almond residues in the range 16–18 MJ kg^{-1} [50], being comparable with the energy content values of lignocellulosic biomass [51]. Friedl et al. [52] compared several heating values (enthalpy of complete combustion of a fuel with all C

converted to CO_2 and all H converted to H_2O) of several bio-mass fuels (wood materials, wood waste, sunflower, energy grass other, hemp, etc.). They found the HHV values in the range 20–15.97 MJ kg^{-1} with carbon contents in the range 50.5–42.6%. These values can be compared to those found for the samples studied in the present work (Table 3), with carbon contents in the range 46–41%). The present values of HHV estimated for waste almond shells are inside this range.

Finally, Demirbaş [53] reported average structural composition of lignocellulosic fuel samples with HHV values in the range 21.53 kJ g^{-1} for olive cake and 17.70 kJ g^{-1} for Tobacco leaf, with 20.05 kJ g^{-1} for halzenut shell, without data for almond shells. This author developed linear equa-tions using the lignin content for the determination of HHV for non-wood, wood and all fuel samples with good correla-tion coefficients (0.9302–0.9658). In the present study, using the prediction equation HHV = 0.0877*x*L + 16.4951 pro-posed by Demirbaş [53] being L the lignin content (14.80% see Table 6), the calculated HHV value is 17.79 kJ g^{-1}. This result can be compared with the average value estimated from other proposed linear equations, as described above.

After this study, it is considered that all these thermal results are of interest in further studies concerning almond shells as waste biomass. A complete kinetic study, using different kinetic models, and the effect of leaching treatment with water will be the next steps in this investigation.

Summary and Conclusions

The almond industry generates large quantities of waste products that need to be recycled or processed. For that rea-son, studies concerning this subject as biomass source are of wide interest. It is generated a large amount of almond shells as waste biomass in the world, being of interest for several potential applications, such as pyrolytic liquid fuels, fuel gas and active carbon. For that reason, it is an important goal to conduct studies to investigate the thermal behav-iour of the different parts of almond shells produced in an almond industry as a waste biomass. In the present study, several experiments have been conducted under laboratory conditions. Although a complete study can be very com-plex, a first approach has been performed in this work. After removing the mature almonds, the waste raw materials were washed with distilled water and separated in several parts taking into account their physical characteristics, as follows: (a) complete shells without grinding (Sample C); (b) ground samples of complete shells, sieved under 0.2 mm (Sample M); (c) hard layers of the endocarp (Sample E); (d) internal layers of the endocarp (Sample I); and (e) mature drupes (Sample P) or skin. The thermal behaviour of all these sam-ple materials has been investigated using a laboratory furnace, with determination of ash contents and weight loss by progressive heating (120 min of holding time). Elemental and DTA-TG/DTG analyses of selected sample materials have been carried out.

Results on thermal decomposition of this biomass waste have been presented and emphasized the main differences between sample materials of almond shells. These results have demonstrated the influence of several parameters, such as previous treatments in the elemental analysis data, the particle size and the different parts of the almond shells, as showed in this investigation. The thermal decomposition of these samples is complex, with mass variations, as detected by a progressive TG increase by heating, overlapping DTG curves and several exothermal DTA effects which must correspond to thermal decomposition and degradation processes of cellulose, hemicellulose and lignin decomposed by progressive heating. However, it is not easy a complete interpretation of the observed thermal evolution and it requires further investigation.

The structural analysis of this waste has been performed. For this purpose, it has been selected a material (Sample M), ground and sieved (under 0.2 mm), similar to that applied in industrial processing of almond wastes. The contents of hemicellulose, cellulose and lignin have been deter-mined. From these results, using the content of lignin, a first approximation for the prediction of the higher heating value (HHV) of this waste as by-product of industrial inter-est has been performed. The average of HHV obtained in this work was 18.24 $MJkg^{-1}$. It was compared with previous results reported in the analysis of biomass plant remains, being the highest value of all these biomass samples. Taking into account the ash contents and the results of elemental analysis, it has been applied some correlations described in the previous research to calculate the HHV values for all the samples. The results obtained are close to the average values of HHV obtained in this work using the lignin content. It is a result of particular interest for a potential application of the almond shell wastes studied in the present investigation.

Acknowledgements The Research Groups AGR 107 and TEP 204 are acknowledged for the financial support of Junta de Andalucía (Regional Government). The company "Llanos del Almendro" from Almería Province (Spain) is acknowledged for waste samples of almond shells. Thanks are extended to Dr. J. Mª Martínez-Blanes (CSIC) for his help to improve the presentation of DTA-TG and TG-DTG curves. This work is dedicated to deceased professor Dr. Manuel Macías Azaña (Department of Inorganic Chemistry, University of Sevilla, Spain) for his broad contribution to thermal analysis and friendship at the thermal laboratory.

References

1. Demirbaş A. Relationships between heating value and lignin, fixed carbon, and volatile material contents of shells from biomass products. Energy Source A. 2003;25:629–35.

2. Demirbaş A. Combustion characteristics of different biomass fuels. Prog Energy Combust Sci. 2004;30:219–30.
3. Demirbaş A. Potential applications of renewable energy sources biomass combustion problems in boiler power systems and combustion related environmental issues. Prog Energy Combust Sci. 2005;31:171–92.
4. Vargas-Moreno JM, Callejón-Ferre AJ, Pérez-Alonso J, et al. A review of the mathematical model for predicting the heating value of biomass materials. Renew Sust Energy Rev. 2012;16:3065–83.
5. Callejón-Ferre AJ, Carreño-Sánchez J, Suárez-Medina FJ, et al. Prediction models for higher heating value based on the structural analysis of the biomass of plants remain from the greenhouses of Almería (Spain). Fuel. 2014;116:377–87.
6. Morales L, Garzón E, Martínez-Blanes JM, Sánchez-Soto PJ. Thermal study of residues from greenhouse crops plant biomass. J Therm Anal Calorim. 2017;129:1111–20.
7. Vassilev S, Baxter D, Andersen L, et al. An overview of the composition and application of biomass ash. Part 1. Phase-mineral and chemical composition and classification. Fuel. 2013;105:40–76.
8. Vassilev S, Baxter D, Andersen L, et al. An overview of the composition and application of biomass ash. Part 2. Poten-tial utilisation, technological and ecological advantages. Fuel. 2013;105:19–39.
9. Cioablă AE, Pop N, Trif-Tordai G, et al. Comparative analysis of agricultural materials influenced by anaerobic fermentation for biogas production in terms of ash melting behaviour. J Therm Anal Calorim. 2017;127:515–23.
10. Magdziarz A, Wilk M. Thermal characteristics of the combustion process of biomass and sewage sludge. J Therm Anal Calorim. 2013;114:519–29.
11. Febrero L, Granada E, Pérez C, Patiño D, Arce E. Characterization and comparison of biomass ashes with different thermal histories using TG-DSC. J Therm Anal Calorim. 2014;118:669–80.
12. Magdziarz A, Dalai AK, Koziński JA. Chemical composi-tion, character and reactivity of renewable fuel ashes. Fuel. 2016;176:135–45.
13. Shah MA, Khan MNS, Kumar V. Biomass residue characterization for their potential application as biofuels. J Therm Anal Calorim. 2018;134:2137–45.
14. Reis JS, Araujo RO, Lima VMR, Queiroz LS, da Costa CEF, Pardauil JRJ, Chaar JS, Rocha Filho GN, de Sousa LKC. Combustion properties of potential Amazon biomass waste for use as fuel. J Therm Anal Calorim. 2019;138:3535–9.
15. Uzoejinwa BB, He X, Wang S, Abomohra AEF, Hu Y, He Z, Wang Q. Co-pyrolysis of macroalgae and lignocellulosic biomass. J Therm Anal Calorim. 2019;136:2001–16.
16. Li Y, Xing X, Ma P, Zhang X, Wu Y, Huang L. Effect of alkali and alkaline earth metals on co-pyrolysis characteristics of munici-pal solid waste and biomass briquettes. J Therm Anal Calorim. 2020;139:489–98.
17. Cruz G, Pereira Rodrigues AL, Ferreira da Silva D, et al. Physical-chemical characterization and thermal behaviour of cassava harvest waste for application in thermochemical processes. J Therm Anal Calorim. 2020. https://doi.org/10.1007/s10973-020-09330-6.
18. Omer AM. Biomass energy resources utilisation and waste management. Agric Sci. 2012;3:124–45.
19. Tripathi N, Hills CD, Singh RS, et al. Biomass waste utilisation in low-carbon products: harnessing a major potential resource. Clim Atmos Change (Nat Partn J). 2019;2:35. https://doi.org/10.1038/s41612-019-0093-5.
20. Lee SY, et al. Waste to bioenergy: a review on the recent conversion technologies. BMC Energy. 2019;1(4):1–22. https://doi.org/10.1186/s42500-019-0004-7.
21. Jenkins BM, Baxter LL, Miles TR, et al. Combustion properties of biomass. Fuel Process Technol. 1998;54:17–46.
22. Khan AA, Jonga WD, Jansen PJ, et al. Biomass combustion in fluidized bed boilers: potential problems and remedies. Fuel Process Technol. 2009;90:21–50.
23. Ni M, Leung DYC, Leung MKH, Sumathy K. An overview of hydrogen production from biomass. Fuel Proc Technol. 2006;87:461–72.
24. Caballero JA, Font R, Marcilla A. Comparative study of the pyrol-ysis of almond shells and their fractions, holocellulose and lignin product yields and ksinetics. Thermochim Acta. 1996;276:57–77.
25. Chiou BS, Cao T, Valenzuela-Medina D, et al. Torrefaction kinet-ics of almond and walnut shells. Effects of inorganic species. J Therm Anal Calorim. 2018;131:3065–75.
26. Regional Government of Andalousie (Junta de Andalucía), Spain. 2016–17. El sector de la almendra en Andalucía. Informe final de la campaña 2016/17. Observatorio de precios y mercados. The sector of almonds in Andalousie. Final report of the campaing 2016/17. Observatory of prices and markets.
27. Rapagna S, Provendier H, Petit C, Kiennemann A, Foscolo PU. Development of catalysts suitable for hydrogen or syn-gas production from biomass gasification. Biomass Bioenergy. 2002;22:377–87.
28. Brown RC. Biomass-derived hydrogen from a thermally ballasted gasifier. FY 2003. Progress Report. National Renewable Energy Laboratory. 2003.
29. Safari F, Javani N, Yumurtaci Z. Hydrogen production via supercritical water gasification of almond shell as catalysts. Int J Hydro-gen Energy. 2018;43:1071–80.
30. Sabbatini A, Lanari S, Santulli C, Pettinari C. Use of almond shells and rice husk as fillers of Poly(Methyl Methacrylate) (PMMA). Compos Mater. 2017;10:1–12.
31. Tasdemir M. Effect of olive pit and almond shell powder on polypropylene. Key Eng Mater. 2017;733:65–8.
32. Maaloul N, Oulego P, Rendueles M, Ghorbal A, Díaz M. Novel biosorbents from almond shells: characterization and adsorption properties modelling for Cu(II) ions from aqueous solutions. J Environ Chem Eng. 2017;5:2944–54.
33. Maaloul N, Ben-Arfi R, Rendueles M, Ghorbal A, Díaz M. Dialysis-free extraction and characterization of cellulose crys-tals from almond (Prunus dulcis) shells. J Mater Environ Sci. 2017;8:4171–81.
34. Cataldo S, Gianguzza A, Milea D, Muratore N, Pettignano A, Sammartano S. A critical approach to the toxic metal ion removed by halzenut and almond shells. Environ Sci Pollution Res. 2018;25:4238–53.
35. Martín-Lara MA, Ortuño N, Conesa JA. Volatile and semivolatile emissions from the pyrolysis of almond shell loaded with heavy metals. Sci Total Environ. 2018;613–614:418–27.
36. Zbair M, Anfar Z, Ait Ahsaine H, El Al-en N, Ezhari M. Acridine orange adsorption by zinc oxide/almond shell activated carbon composite: operational factors, mechanism and performance optimization using central composite design and surface modelling. J Environ Manag. 2018;206:383–97.
37. Moussa I, Baaka N, Kihiari R, Moussa A, Mortha G, Farouk M. Application of Prunus amygdalus By-products in Eco-friendly Dyening of textile fabrics. J Renew Mater. 2018;6:55–67.
38. Chen P, Cheng Y, Deng S, Lin X, Huang G, Ruan R. Utilization of almond residues. Int J Agric Biol Eng. 2010;3:1–18.
39. Allouch M, Boukhlifi F, Alami M. Study of the Thermal Behavior of Almond Shells and Acorn Cups for Production of Fuel Briquettes. Energy Tecnol Policy. 2014;4:33–9.
40. Li X, Hao J, Wang W. Study of Almond Shell Characteristics. Mater. 2018;11:1782. https://doi.org/10.3390/ma11091782.
41. Strezov V, Moghtadevi B, Lucas JA. Thermal study of decomposition of selected biomass samples. J Therm Anal Calorim. 2003;72:1041–8.

42. Telmo C, Lousada J, Moreira N. Proximate analysis, backwards stepwise regression between gros calorific value, ultimate and chemical analysis of wood. Bioresour Technol. 2010;101:3808–15.
43. Van Soest PJ, Robertson JB, Lewis BA. Methods for dietary fiber, neutral detergent fiber and nonstarch polysaccharides in relation to animal nutrition. J Dairy Sci. 1991;74:3583–97.
44. Yildiz S. Kinetic and isotherm analysis of Cu(II) adsorption onto almond shell (Prunus dulcis). Ecol Chem Eng Sci. 2017;24:87–106.
45. Callejón-Ferre AJ, Velázquez-Martí B, López-Martínez JA, Manzano-Augliaro F. Greenhouse crop residues: energy potential and models for the prediction of their higher heating value. Renew Sust Energy Rev. 2011;15:948–55.
46. Demirbaş A. Calculation of higher heating values of biomass fuels. Fuel. 1997;76:431–4.
47. Sheng C, Azevedo JLT. Estimating the higher heating value of biomass fuels from basic analysis data. Biomass Bioener. 2005;28:499–507.
48. Erol M, Haykiri-Acma H, Kücükbayrak S. Calorific value estimation of biomass from their proximate analyses data. Renew Energy. 2010;35:170–3.
49. Channiwala SA, Parikh PP. A unified correlation for estimating HHV of solid, liquid and gaseous fuels. Fuel. 2002;81:1051–63.
50. González J, Gañán J, Ramiro A, González-García CM, Encinar JM, Sabio E. Almond residues gasification plant for generation of electric power. Prelim Study Fuel Process Technol. 2006;87:149–55.
51. McKendry P. Energy production from biomass (part 1): overview of biomass. Biores Technol. 2002;83:37–46.
52. Friedl A, Padouvas E, Rotter H, Varmuza K. Prediction heating values of biomass fuel from elemental composition. An Chim Acta. 2005;544:191–8.
53. Demirbaş A. Relationships between lignin contents and heating values of biomass. Energy Convers Manage. 2001;42:183–8.